Current Applied Physics 9 (2009) 972–977

Contents lists available at ScienceDirect

Current Applied Physics

journal homepage: www.elsevier.com/locate/cap

Current–voltage–temperature (*I–V–T*) characteristics of Pd/Au Schottky contacts on n-InP (1 1 1)

M. Bhaskar Reddy, A. Ashok Kumar, V. Janardhanam, V. Rajagopal Reddy *, P. Narasimha Reddy

Department of Physics, Sri Venkateswara University, Tirupati-517 502, India

ARTICLE INFO

Article history:
Received 19 July 2008
Received in revised form 2 September 2008
Accepted 8 October 2008
Available online 17 October 2008

PACS:
73.30.+y
73.40.Ei
73.40.Ns
73.40.Sx

Keywords:
Current–voltage–temperature characteristics
Schottky barrier height
Pd/Au Schottky contact
n-Type InP

ABSTRACT

We have investigated the current–voltage–temperature (*I–V–T*) characteristics of Pd/Au/InP Schottky barrier diodes in the temperature range of 220–400 K. The *I–V* analysis based on thermionic emission (TE) theory shows an abnormal decrease of apparent barrier height and increase of ideality factor at low temperatures. The conventional Richardson plot exhibits nonlinearity with activation energy of 0.17 eV and the Richardson constant value of 5.63×10^{-6} A cm^{-2} K^{-2}. The nonlinearity in the Richardson plot and strong dependence of Schottky barrier parameters on temperature may be attributed to the spatial inhomogeneity in the interface. Further, the homogeneous barrier height has been obtained from the linear relationship between experimentally obtained effective barrier heights and ideality factors. Φ_b versus $(2kT)^{-1}$ plot has been drawn to obtain the mean barrier height $[\bar{\Phi}_{bo}(T = 0\ \mathrm{K})]$ and the standard deviation (σ_s) at zero-bias which are found to be 0.84 eV, 138 meV, respectively. The series resistance is also estimated from the forward current–voltage characteristics of Pd/Au/InP Schottky contacts using Cheung's method and found that it is strongly dependent on temperature and also decreases with increase in temperature.

1. Introduction

Indium phosphide (InP) is an attractive III–V compound semiconductor which finds wide applications in optoelectronic and high speed electronic devices due to a direct bandgap and high electron mobility [1–4]. Metal–semiconductor structures especially Schottky contacts play key role in making new semiconductor devices. However, a serious limitation of InP Schottky barrier diodes (SBD) is the low barrier height (BH) and large leakage currents which may be due to Fermi level pinning. However, SBDs with low barrier height find applications in devices operating at cryogenic temperatures as infrared detectors and sensors in thermal imaging [5,6].

The current–voltage characteristics of the Schottky diodes obtained at room temperature does not give detailed information about the charge transport process and the nature of the barrier formed at metal–semiconductor interface. The temperature-dependent electrical characteristics of the Schottky contacts provide the information regarding the charge transport process through metal–semiconductor contacts and also give a better picture of the conduction mechanisms. Schottky contacts often show anomalous temperature-dependent behaviour as evidenced by the parameters such as ideality factor, barrier height and series resistance. Analysis of the *I–V* characteristics of Schottky barrier diodes based on thermionic emission theory usually reveals an abnormal variations in barrier height (Φ_{bo}) and in ideality factor with decrease in temperature [7–10]. The observed current–voltage characteristics of the Schottky barrier diode usually deviate from the ideal thermionic emission (TE) model. This could be due to the strong dependence of both barrier height and ideality factor on temperature and the nonlinearity of the Richardson plots [11–14]. Any decrease in barrier height at low temperature leads to nonlinearity in the activation energy plot i.e., $\ln(I_0/T^2)$ versus $1000/T$. The deviation in TE model observed in *I–V* characteristics could be quantitatively explained by assuming specific distribution of nanometer scale patches of small regions with low barrier heights embedded in a high uniform barrier height background [15–17].

Several researchers have studied temperature-dependent characteristics of Schottky contacts on n-type InP [18–21]. Cetin and Ayyildiz [18] studied temperature dependence of electrical characteristics of Au/InP Schottky barrier diode. They observed that the ideality factor decreases while the barrier height increases with

* Corresponding author.
E-mail address: reddy_vrg@rediffmail.com (V. Rajagopal Reddy).

1567-1739/$ - see front matter © 2008 Elsevier B.V. All rights reserved.
doi:10.1016/j.cap.2008.10.001

increase of temperature. Cimilli et al. [19] fabricated Au/n-InP/In Schottky barrier diodes, and reported that the barrier height varied from 0.557 to 0.615 eV and the ideality factor from 1.002 to 1.087. Recently, Ashok et al. [20] studied the current–voltage–temperature (I–V–T) characteristics of Pd/InP Schottky diodes and found that the barrier parameters vary significantly with temperature. More recently, Cimilli et al. [21] investigated the temperature-dependent electrical properties Ag/n-InP/In Schottky diodes in a wide temperature range (30–320 K). In the present work, we report on the current–voltage–temperature (I–V–T) characteristics of Pd/Au/InP Schottky diodes in the temperature range of 220–400 K.

2. Experimental details

Liquid Encapsulated Czokralski (LEC) grown undoped n-InP (1 1 1) samples with carrier concentration of 4.5×10^{15} cm^{-3} are used in the present work. The samples are initially degreased with organic solvents like trichloroethylene, acetone and methanol by means of ultrasonic agitation for 5 min in each stage to remove contaminants followed by rinsing in deionised water and then dried in N_2 flow. The samples are then etched with HF (49%) and H_2O (1:10) to remove the native oxides from the substrate. Indium ohmic contacts of thickness 500 Å are formed on the rough side of the InP wafer prior to Schottky diode fabrication at a pressure of 7×10^{-6} mbar which are then annealed at 350 °C for 1 min in N_2 atmosphere. For making Schottky contacts, the metals Pd/Au of 500 Å each using mask of diameter 0.7 mm are deposited on the polished side of InP wafer. The current–voltage (I–V) characteristics of the as-deposited Pd/Au/n-InP Schottky diodes are measured in the temperature range of 220–400 K by automated DLS-83D spectrometer (Semi Lab, Hungary).

3. Results and discussion

Fig. 1 shows the typical forward and reverse current–voltage characteristics of Pd/Au/n-InP Schottky diodes in the temperature range of 220–400 K. For Schottky diode, the thermionic emission theory predicts that the current–voltage characteristic is given by [4],

$$I = I_S\left[\exp\left(\frac{qV}{nkT}\right) - 1\right], \tag{1}$$

$$\text{where} \quad I_S = AA^*T^2\exp\left[-\frac{q\Phi_b}{kT}\right], \tag{2}$$

where I_S is the reverse saturation current, q is the electron charge, V is the applied voltage and n is the ideality factor where

$$n = \frac{q}{kT}\left[\frac{dV}{d(\ln I)}\right], \tag{3}$$

A is the diode area, A^* is the effective Richardson constant and Φ_b is the Schottky barrier height. The value of Φ_b can be deduced from the I–V curves with known value of Richardson constant A^*. The calculated value of A^* is 9.4 A cm^{-2} K^{-2} based on the effective mass ($m^* = 0.078\ m_o$) of n-InP [22]. The value of I_S is found from the intercept of a plot of $I/[1-\exp(-qV/kT)]$ versus V for the temperature range of 220–400 K (Fig. 2) and its value is used to determine the barrier height for the contacts. The ideality factor is obtained from the linear portions of the plot between natural log of current and voltage over two orders of magnitude. The value of the BH and ideality factor are varied from 0.35 eV and 2.14 at 220 K to 0.57 eV and 1.42 at 400 K, respectively as shown in Fig. 3. It is observed that the barrier height is increased linearly with increase in temperature from 220–400 K. Fig. 4 is the plot of ideality factor versus temperature which shows the increase of ideality factor with decrease of temperature.

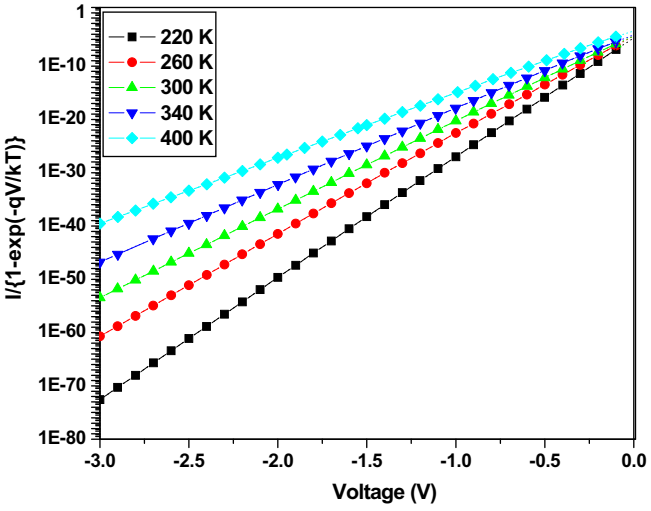

Fig. 2. Plot of $I/[1-\exp(-qV/kT)]$ against V for the Pd/Au Schottky diode.

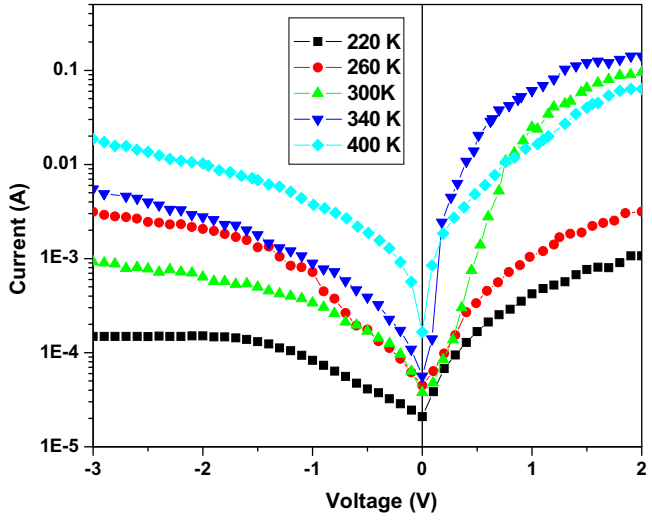

Fig. 1. Typical current–voltage characteristics of Pd/Au Schottky diode in the temperature range of 220–400 K.

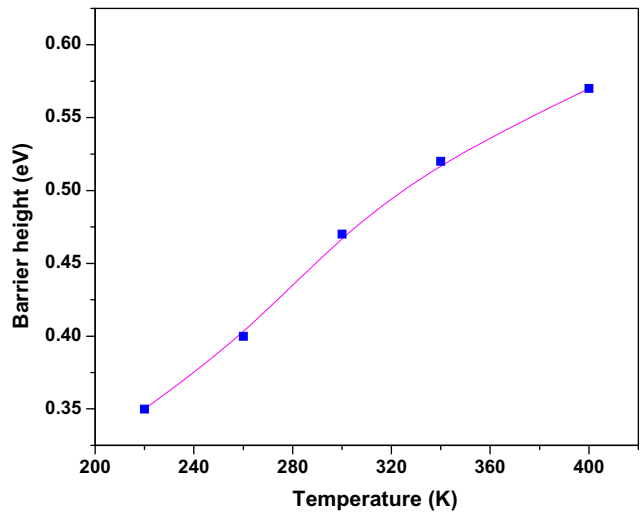

Fig. 3. Plot of Schottky barrier height against temperature for Pd/Au Schottky diode.

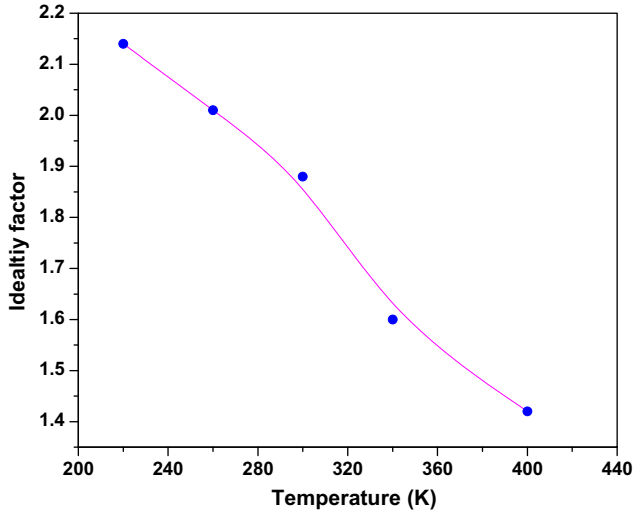

Fig. 4. Plot of ideality factor versus temperature for Pd/Au Schottky diode.

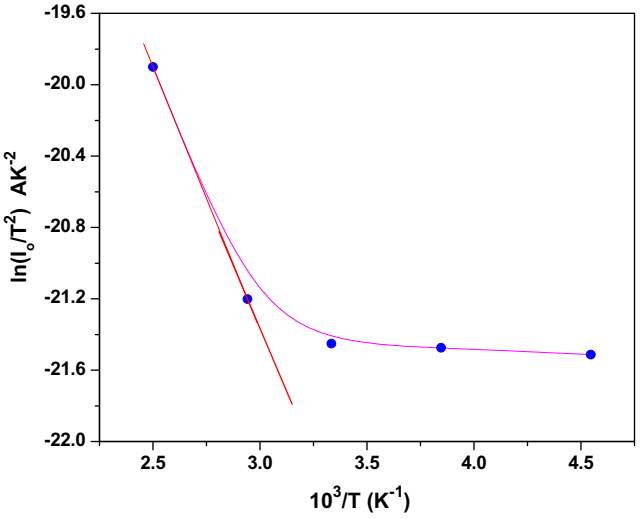

Fig. 5. Richardson plot of $\ln(I_0/T^2)$ against $10^3/T$ for Pd/Au Schottky diode.

The decrease in the barrier height and increase in the ideality factor with decrease in temperature are observed from current–voltage characteristics of Pd/Au Schottky contacts. It may be due to the discontinuities at the interface which may exist even for well controlled fabrication of the sample. Many models have been evolved to explain the inhomogeneity in the barrier [17,23,24]. Tung [17] proposed a potential fluctuation model to explain the inhomogeneity in the barrier height which shows a larger deviation from the classical thermionic theory at low temperature. Based on the results of Werner and Guttler [13], the potential fluctuation model has been effectively used to explain the temperature-dependent results of Schottky contacts.

Due to the inhomogeneity, charge transport across the interface is no longer due to thermionic emission because of presence of nanometer scale interfacial patches of small regions with low barrier heights embedded in a higher background uniform barrier [17]. Since current transport across the interface is temperature-activated process, electrons are able to overcome the lower barriers; the current transport will be dominated by current flowing through the patches of lower barrier height and have large ideality factor. According to potential fluctuation model, at sufficiently low temperatures, a large number of patches may be present and consequently, the current will be dominated by the flow through these patches. As the temperature increases, more and more electrons may have sufficient energy to overcome the high barriers. As a result both the barrier height and ideality factor observed from temperature-dependent I–V characteristics are consistent with SBH inhomogeneity.

The Richardson plot drawn between $\ln(I_S/T^2)$ and $10^3/T$ used to obtain the zero-bias barrier height and Richardson constant is shown in Fig. 5. Eq. (2) can be rewritten as,

$$\ln\left(\frac{I_S}{T^2}\right) = \ln(AA^*) - \frac{q\Phi_b}{kT}. \tag{4}$$

From Eq. (4), the plot $\ln(I_S/T^2)$ versus $10^3/T$ is a straight line whose slope gives the barrier height at 0 K and the intercept gives the Richardson constant. The value of A^* obtained from the intercept of the linear portion of the ordinate is 5.63×10^{-6} A cm^{-2} K^{-2}, which is much lower than the known value of 9.4 A cm^{-2} K^{-2}. A barrier height value of 0.17 eV is obtained from the slope of the straight line. The bowing of the experimental $\ln(I_S/T^2)$ versus $1/T$ plot is caused by the temperature dependence of the barrier height. The obtained value of A^* is low since it is calculated from the temperature-dependent I–V characteristics which may be affected by lateral inhomogeneity of the barrier. A^* is also different from the theoretical value since its value depends on the value of the real effective mass that it is different from the calculated one according to Horvath [25]. The decrease in barrier height at low temperatures leads to nonlinearity in the activation energy [$\ln(I_S/T^2)$ versus $1/T$] plot. The nonlinearity in the Richardson plot may be due to spatially inhomogeneous barrier height and potential fluctuation at the interface that consists of low and high barrier areas, that is, the current through the diode will flow preferentially through the low barriers in the potential distribution [17,23]. The results obtained are in consistent with the potential fluctuation model.

In using the Richardson plot to obtain Φ_b and A^*, the current transport mechanism must be primarily due to thermoionic emission. If this was not the case, the Richardson plot would yield erroneous results. Furthermore, the thermoionic emission transport mechanism requires that the ideality factor be a constant for different temperatures and close to 1.0. At low temperature, the ideality factor is characterized by the current flow through the distribution of low-Schottky barrier height patches since the ideality factor is defined as the ideality factor of large uniform region by approaching unity at high temperatures. As the temperature increases, the lower effective barrier height of the patches is offset by the much greater area of the uniform region. As a result, most current flows through the uniform region which may improve the ideality factor at high temperature and the current transport mechanism is dominant by thermoionic emission.

3.1. Barrier height variation with ideality factor

The variation of ideality factor and barrier height with respect to temperature is due to the inhomogeneities in the interface. Schmitsdorf et al. [26] used Tung's theoretical approach and they found a linear correlation between the experimental zero-bias barrier height and the ideality factor. The barrier height decreases as the ideality factor increases as shown in Fig. 6. The straight line plot is the least square fit of the experimental data which indicates a linear relationship between experimental effective barrier height and ideality factor of Schottky contacts and is attributed to lateral inhomogeneities of the barrier heights in the Schottky diodes. An apparent decrease in barrier height and increase in ideality factor at low temperature are possibly caused by some other effects such as inhomogeneities in thickness and composition of the layer,

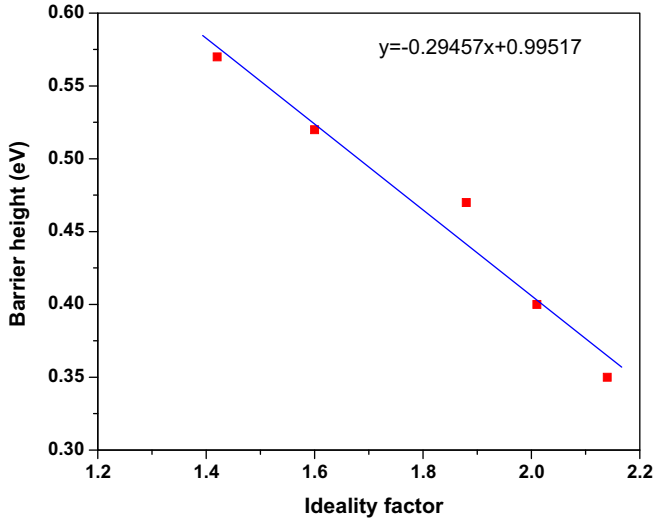

Fig. 6. Zero-bias apparent barrier height versus ideality factor of Pd/Au Schottky diode.

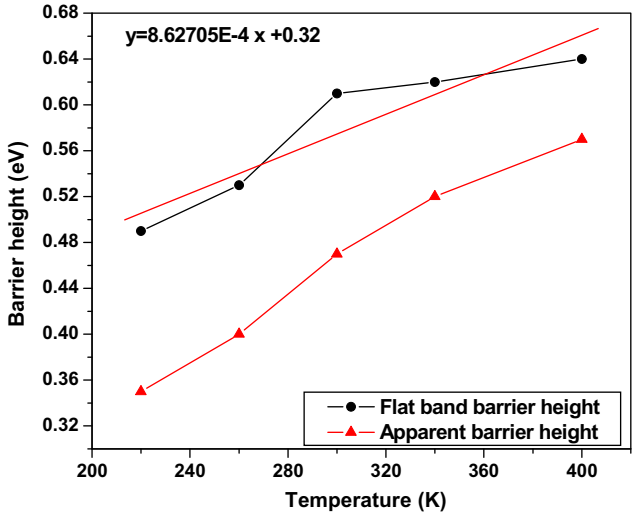

Fig. 7. Plot of variation of the flat-band barrier height with temperature for Pd/Au Schottky diode.

non-uniformity of the interfacial charges or the presence of a thin insulating layer between the metal and the semiconductor [27,28]. At low temperature, the current will be dominated by the current through the patches of low barrier heights because the current transport across the metal–semiconductor interface is a temperature-activated process.

The extrapolation of the experimental barrier height versus ideality factor plot to $n = 1$ gives a homogeneous barrier height (Φ_b^{hom}) of approximately 0.99 eV. Thus, it is noticed that the significant decrease of the zero-bias barrier height and increase of the ideality factor especially at low temperature may be due to barrier inhomogeneities. According to the model of Tung [17], this value should represent the barrier height of the ideal homogeneous contact i.e., the highest value of the barrier height distribution in which small patches of lower barrier is embedded.

3.2. Variation of flat-band barrier height with temperature

The barrier height obtained from Eq. (2) is called as apparent or zero-bias barrier height. It increases with increasing of temperature of Schottky contact depending on the electric field across the contact, and consequently on the applied bias voltage. The variation of flat-band barrier height of the Pd/Au/n-InP Schottky barrier diodes calculated from the current–voltage barrier heights and the corresponding ideality factor at each temperature is shown in the Fig. 7. However, the barrier height obtained under flat-band condition is considered to be real quantity. Unlike the case of zero-bias barrier height, the electric field is zero under flat-band condition. This eliminates the effect of the image force lowering that would affect the current–voltage characteristics and removes the influence of lateral inhomogeneity [29].

By using Eq. (5), the flat-band barrier height Φ_{bf} can be calculated using the experimental ideality factor and zero-bias barrier height Φ_{bo} [30].

$$\Phi_{bf} = n\Phi_{bo} - (n-1)\frac{kT}{q}\ln\left(\frac{N_C}{N_D}\right), \tag{5}$$

where N_C is the density of states in the conduction band and N_D is the donor concentration. The temperature-dependent values of N_C and N_D are used in calculating Φ_{bf} values. The Φ_{bf} increases with increase in temperature in the temperature range of 220–400 K (Fig. 7). The temperature dependence of flat-band barrier height can be expressed as,

$$\Phi_{bf}(T) = \Phi_{bf}(T = 0\ \mathrm{K}) + \alpha T, \tag{6}$$

where Φ_{bf} ($T = 0$ K) is the flat-band barrier height extrapolated to 0 K and α is the temperature coefficient. From the slope and intercept of the least square fit of the Φ_{bf} (T) data in the temperature range of 220–400 K give the values of Φ_{bf} and α. The values obtained are Φ_{bf} ($T = 0$ K) is 0.32 eV and α is 8.62705×10^{-4} eV/K.

3.3. Temperature-dependent of series resistance

Temperature dependence of series resistance affects the electrical properties of the Pd/Au/InP Schottky diode and is measured in the temperature range of 220–400 K. In general, the forward bias current–voltage characteristics are linear on a semi logarithmic scale at low forward bias voltages but deviate considerably from linearity due to the effect of series resistance R_S and other effects.

The series resistance values are evaluated from the forward bias current–voltage data using the method developed by Cheung [31]. The forward bias current–voltage characteristics due to thermionic emission of a Schottky contact with the series resistance can be expressed as Cheung's function given by,

$$\frac{dV}{d(\ln I)} = IR_S + n\left(\frac{kT}{q}\right). \tag{7}$$

The plots of experimental $dV/d(\ln I)$ versus I for different temperatures are shown in Fig. 8. The series resistance value R_S is obtained from the slope and nkT/q value from the y-intercept. The series resistance decreases with increase in temperature. It is observed that the decrease in series resistance is more at low temperatures than at high temperatures since the slope of the curve is large at low temperatures (Fig. 9). The variation of R_S with temperature may be due to the factors responsible for the increase in ideality factor n and lack of free carrier concentration at low temperatures [32]. The barrier heights, ideality factors and series resistance of the Pd/Au Schottky contact as a function of temperature are given in Table 1.

3.4. Analysis of inhomogeneous barrier height

The abnormal deviations of current–voltage characteristics of the Schottky diode from the classical thermionic emission theory can also be explained by the lateral distribution of barrier height if the barrier height has a Gaussian distribution. The Gaussian

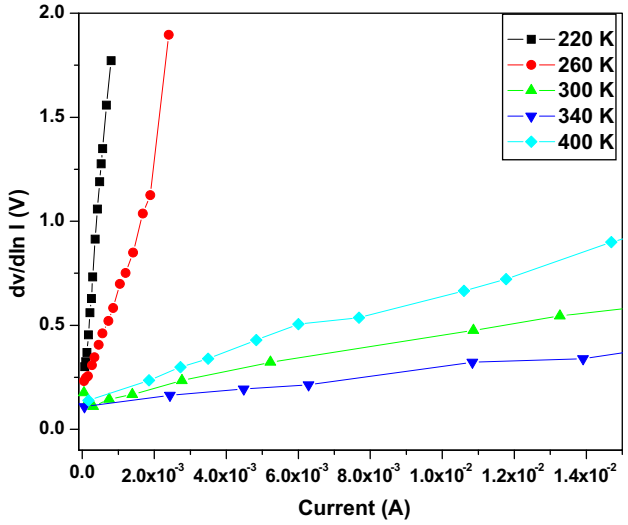

Fig. 8. Plots of dV/dln (I) versus current (I) for Pd/Au Schottky contacts at various temperatures.

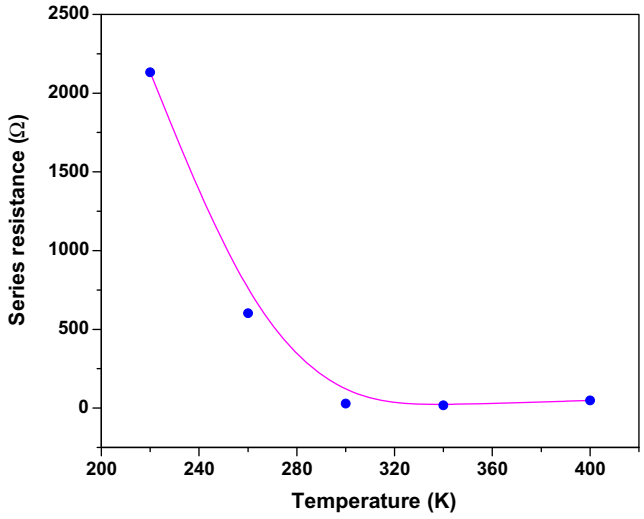

Fig. 9. Temperature dependence of the series resistance for Pd/Au Schottky diode.

distribution of barrier heights over the Schottky contact area can be explained with the mean barrier height $\overline{\Phi_{bo}}(T = 0\ \mathrm{K})$ and standard deviation σ_0. The standard deviation is a measure of the barrier homogeneity. According to Gaussian distribution, the expression for the barrier height is given by [33,34],

$$\Phi_b = \overline{\Phi}_b(T = 0\ \mathrm{K}) - \frac{q\sigma_0^2}{2kT}, \tag{8}$$

where Φ_b is the apparent barrier height measured experimentally. The temperature dependence of σ_0 is usually small and can be neglected. The observed variation of ideality factor with temperature in the model is given by [13],

$$\left(\frac{1}{n_{ap}} - 1\right) = -\rho_2 + \frac{q\rho_3}{2kT}, \tag{9}$$

where n_{ap} is apparent ideality factor (experimental data) and ρ_2 and ρ_3 quantify the voltage deformation of the barrier height distribution. The experimental Φ_b versus $1/2kT$ and n_{ap} versus $1/2kT$ plots are shown in Fig. 10. The linearity in the apparent barrier height (experimental data) or ideality factor versus $1/2kT$ curves is in

Table 1
The barrier heights, ideality factors and series resistance of the Pd/Au Schottky contact as a function of temperature.

Temperature (K)	Barrier height (eV)	Ideality factor	Series resistance (Ω)
220	0.35	2.14	2133
260	0.40	2.01	603
300	0.47	1.88	29
340	0.52	1.6	18
400	0.57	1.42	49

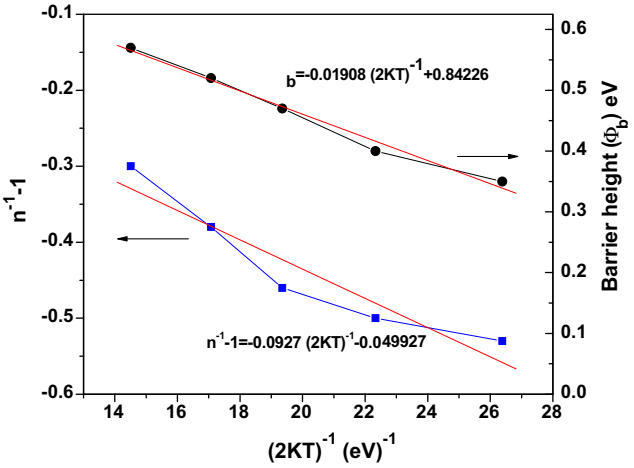

Fig. 10. Zero-bias apparent barrier height and ideality factor versus $(2kT)^{-1}$ curves of the Pd/Au/InP Schottky diode according to the Gaussian barrier height.

agreement with the recent model which is related to thermionic emission over a Gaussian distribution. The plot of Φ_b versus $1/2kT$ is a straight line with the intercept on the ordinate determining the zero mean barrier height $\overline{\Phi_{bo}}(T = 0\ \mathrm{K})$ and the slope gives the zero-bias standard deviation σ_0. The values obtained are 0.84 eV and 138 meV respectively for $\overline{\Phi_{bo}}(T = 0K)$ and σ_0 respectively.

The experimental ideality factor versus $1/2kT$ plot is a straight line. The values obtained for ρ_2 and ρ_3 from the intercept and the slope of the straight line are 0.0927 and −0.049927, respectively. The linear behaviour of this plot demonstrates that the ideality factor explains the voltage deformation of the Gaussian distribution of the Schottky barrier height. The lower value of σ_0 corresponds to more homogeneous barrier heights. According to Calvet et al. [35], the value of σ_0 (138 meV) is not small compared to the mean value of $\overline{\Phi_{bo}}(T = 0\ \mathrm{K})$ which is 0.84 eV which indicates the greater inhomogeneities at the interface and thus potential fluctuation. The inhomogeneity and potential fluctuation only affect low temperature current–voltage characteristics.

4. Conclusion

We report on the temperature-dependent I–V characteristics of the Pd/Au/n-InP Schottky diodes in the temperature range of 220–400 K. The obtained I–V barrier heights are in the range of 0.35–0.57 eV and that of ideality factor are 2.14–1.42. The obtained Schottky diode parameters such as ideality factor, barrier height and series resistance from forward I–V characteristics shows strong dependence on temperature. The increase in ideality factor and decrease in barrier height with decrease in temperature have been successfully explained based on the thermionic emission with the assumption of Gaussian distribution of the barrier heights at the interface. The nonlinearity in the Richardson plot gives a clear indication of the inhomogeneity in the barrier height. The homogeneous barrier height (Φ_b^{hom}) of approximately 0.99 eV has been

obtained from the linear relationship between experimental barrier heights and ideality factor. The extracted value of mean barrier height and standard deviation clearly indicates the presence of interface inhomogeneities and potential fluctuation at the interface.

References

[1] E.H. Rhoderick, R.H. Williams, Metal–Semiconductor Contacts, second ed., Clarendon, Oxford, 1988.
[2] H.K. Henisch, Semiconductor Contacts, Oxford University, London, 1984.
[3] R.T. Tung, Mater. Sci. Eng. R 35 (2001) 1.
[4] C.W. Wilmsen, Physics and Chemistry of III–V Compound Semiconductor Interfaces, Plenum, New York, 1985.
[5] P.G. Mc Cafferty, A. Sellai, P. Dawson, H. Elasd, Solid-State Electron. 39 (1996) 583.
[6] S. Chand, J. Kumar, Appl. Phys. A 63 (1996) 471.
[7] S. Chand, J. Kumar, Semicond. Sci. Technol. 10 (1995) 1680.
[8] S. Karatas, S. Altindal, M. Caskar, Physica B 357 (2005) 373.
[9] R. Hackam, P. Horrop, IEEE Trans. Electron. Dev. 19 (1972) 1231.
[10] A.S. Bhuiyan, A. Martinez, D. Esteve, Thin Solid Films 161 (1988) 93.
[11] I. Dokmee, S. Altindal, Semicond. Sci. Technol. 21 (2006) 1053.
[12] Y.P. Song, R.L. Van Meirhaeghe, W.H. Laflere, P. Cardon, Solid-State Electron. 29 (1986) 633.
[13] (a) J.H. Werner, H.H. Guttler, J. Appl. Phys. 69 (1991) 1522;
(b) J.H. Werner, H.H. Guttler, J. Appl. Phys. 73 (1993) 1315.
[14] A. Gumus, A. Trust, N. Yalcin, J. Appl. Phys. 91 (2002) 245.
[15] S. Bandyopadyay, A. Battacharya, S.K. Sen, J. Appl. Phys. 85 (1991) 3671.
[16] M.C. Lonergan, F.E. Zones, J. Chem. Phys. 115 (2001) 433.
[17] R.T. Tung, Phys. Rev. B 45 (1992) 13509.
[18] H. Cetin, E. Ayyildiz, Semicond. Sci. Technol. 20 (2005) 625.
[19] F.E. Cimilli, M. Saglam, A. Turut, Semicond. Sci. Technol. 22 (2007) 851.
[20] A. Ashok Kumar, V. Janardhanam, V. Rajagopal Reddy, P. Narasimha Reddy, J. Optoelectron. Advan. Mater. 9 (2007) 3877.
[21] F.E. Cimilli, H. Efeoglu, M. Saglam, A. Turut, J. Mater. Sci.: Mater. Electron, in press.
[22] K. Hattori, Y. Torii, Solid-State Electron. 34 (1991) 527.
[23] J.D. Levine, J. Appl. Phys. 42 (1971) 3991.
[24] F.A. Padovani, R. Stratton, Solid-State Electron. 9 (1996) 695.
[25] Zs.J. Horvath, Solid-State Electron. 39 (1996) 176.
[26] R.F. Schmitsdorf, T.U. Kampen, W. Monch, J. Vac. Sci. Technol. B 15 (1997) 1221.
[27] S. Zhu, R.L. Meirhaeghe, S. Forment, G.P. Ru, X.P. Qu, B.Z. Li, Solid-State Electron. 48 (2004) 1205.
[28] S. Karatas, S. Altindal, A. Turut, A. Ozmen, Appl. Surf. Sci. 217 (2003) 250.
[29] S. Hardikar, M.K. Hudait, P. Modak, S.B. Krupanidhi, N. Padha, Appl. Phys. A 68 (1999) 49.
[30] F. Wegner, R.W. Young, A. Sugermen, IEEE Electron. Dev. Lett. 4 (1983) 320.
[31] K. Cheung, N.W. Cheung, Appl. Phys. Lett. 49 (1986) 85.
[32] S. Chand, J. Kumar, J. Appl. Phys. 80 (1996) 288.
[33] J. Osvald, Zs.J. Horvath, Appl. Surf. Sci. 234 (2004) 349.
[34] S. Chand, S. Bala, Appl. Surf. Sci. 252 (2005) 358.
[35] E. Cavlet, R.G. Wheeler, M.A. Reed, Appl. Phys. Lett. 80 (2002) 1761.